Mid-infrared microspectroscopic imaging with a quantum cascade laser

Kevin Yeh[a], Matthew Schulmerich[a], and Rohit Bhargava[a,b,*]
[a] Department of Bioengineering and Beckman Institute for Advanced Science and Technology
[b] Departments of Electrical and Computer Engineering, Mechanical Science and Engineering, Chemical and Biomolecular Engineering and University of Illinois Cancer Center
University of Illinois at Urbana-Champaign, Urbana, IL 61801, USA

ABSTRACT

Conventional mid-infrared (mid-IR) Fourier transform infrared (FT-IR) spectroscopic imaging systems employ an incoherent globar source and achieve spectral contrast through interferometry. While this approach is suitable for many general applications, recent advancements in broadly tunable external cavity Quantum Cascade Lasers (QCL) offer new approaches to and new possibilities for mid-IR micro-spectroscopic imaging. While QCL-based devices have yet to achieve the wide spectral range generally employed by spectroscopists for molecular analyses, they are starting to be used for microscopy at discrete frequencies. Here, we present a discrete frequency IR (DFIR) microscope based on a QCL source and explore its utility for mid-IR imaging. In our prototype instrument, spectral contrast is achieved by tuning the QCL to bands in a narrow spectral region of interest. We demonstrate wide-field imaging employing a 128x128 pixel liquid nitrogen cooled mercury cadmium telluride (MCT) focal plane array (FPA) detector. The resulting images demonstrate successful imaging as well as several unique features due to coherence effects from the laser source. Here we discuss the effects of this coherence and compare our instrument to conventional mid-IR imaging instrumentation.

Keywords: Mid-infrared spectroscopy, Quantum Cascade Laser (QCL), Fourier transform infrared (FT-IR), chemical imaging, microscopy, discrete frequency infrared (DFIR)

1. INTRODUCTION

Infrared (IR) spectroscopic microscopy is a widely-used technology for achieving chemical contrast at the micrometer scale. Modern instrumentation combines mid-infrared vibrational spectroscopy, microscopy and wide-field detection[1] and has been shown to have broad applications, including in polymer science,[2] cancer histopathology,[3] drug diffusion studies,[4] analyses of trace gasses,[5] and tissue engineering.[6] The basis of this approach relies on the property that many functional groups in molecules have resonant frequencies in the mid-IR spectral range (2-14 μm). The absorption spectrum is a chemical signature that contains contributions from each of the different functional groups constituting the molecules and can be used to create contrast in the image thus providing direct material identification and alleviating the need for external contrast agents or chemical dyes.

One approach to chemical imaging is Fourier transform infrared (FT-IR) spectroscopy. The powerful advantage of FT-IR spectrometry for imaging is in the ability to multiplex signals via interferometry, which allows for the full intensity of the source to be used at all wavelengths therefore resulting in a multi-fold advantage in sensitivity and resolving power when compared to other methods of achieving spectral resolution.[7] FT-IR spectrometers typically employ a globar thermal source which is simple, stable, and low cost. Its broadband emission profile has sufficient intensity for many applications. The most recent improvements in IR spectroscopic imaging continue to be driven by the development of larger format multiple-element linear and focal plane array (FPA) detectors, which require use in a careful manner.[8] Dividing the total flux of a globar source over an increasing number of detector array elements is a system limitation; therefore, higher flux sources have potential to offer major improvements in imaging performance. The use of a synchrotron source,[9] for example, has enabled faster high-definition IR imaging compared to a laboratory setup.[10]

* Corresponding author. E-mail: rxb@illinois.edu. Address: 4265 Beckman Institute, University of Illinois at Urbana-Champaign, 405 N. Mathews Avenue, Urbana, IL 61801. Tel: (217) 265-6596

Next-Generation Spectroscopic Technologies VI, edited by Mark A. Druy, Richard A. Crocombe, Proc. of SPIE Vol. 8726, 87260E · © 2013 SPIE
CCC code: 0277-786X/13/$18 · doi: 10.1117/12.2015984

Quantum Cascade Lasers (QCL), first developed in the 1990s,[11] are now becoming commercially available in a variety of packaging options and wavelength regions. They are often designed as an external-cavity laser that utilizes an adjustable grating for spectral selection of tunable discrete frequencies (DF).[12] QCLs can emit extremely narrow spectral line widths less than 0.01cm^{-1} with wavelength dependent intensities averaging over 100mW, far exceeding that put out by a globar source, while functioning at room temperature in a comparatively compact package.[13] Additionally, newer QCL models are rapidly being developed with larger tunable ranges.[14] QCLs have been reported in a variety of studies investigating their use in IR spectroscopic analysis,[15,16,17,18] microscopy,[19] and imaging.[20,21]

While there are examples of using lasers for spectroscopic imaging, these are usually prevalent at either macro (> 1 mm) or nanoscale (~ 10 nm) resolution. The ratio of the wavelength to feature size, hence, is either very large or very small in these cases. Wide-field microscopic imaging in the mid-IR using a coherent laser source, where the feature sizes in the image are approximately of the same order of magnitude as the wavelength, presents new challenges.[19] While challenges in understanding data in a microscope using an incoherent source have been recently addressed,[22,23,24] the spatial coherence in using QCLs will require careful interpretation of the data. In particular, the introduction of interference patterns that will appear as either laser speckle or edge fringing caused by the physical structures in the sample, need to be carefully understood. Furthermore, the tunable range of a single QCL only covers a relatively small region of the mid-IR spectrum. In order for meaningful spectroscopic analysis of tissues and other materials, multiple QCL units will be needed to cover the spectral range typically utilized in FT-IR spectroscopy. Accuracy and stability in beam tuning and power output will also be important areas of investigation. In this manuscript, we report on our initial efforts to characterize and demonstrate the feasibility of QCL sources for discrete frequency infrared spectroscopy and microscopy.

2. EXPERIMENTAL

2.1 Instrumentation

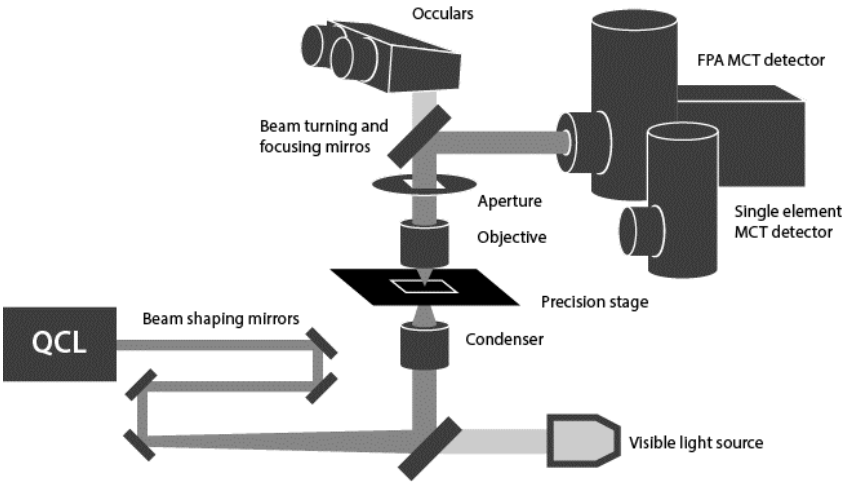

Figure 1. Schematic of the QCL-based wide field imaging components configured in transmission mode

The instrument we have developed in-house is schematically illustrated in Figure 1. It uses a tunable QCL (Daylight Solutions, San Diego, CA), operable in continuous wave (CW) or pulsed modes, with a frequency tuning range between 1570 to 1738 cm^{-1}, wavelength dependent power typically over 100 mW, and a laser linewidth of 0.003 cm^{-1}. Water cooling maintains the laser at its optimal operating temperature of under 20° Celsius. The laser output is expanded to fill the back aperture of the condenser via a series of optical elements. The optical system is comprised of a 0.56 NA germanium glass alloy ($Ge_{28}Sb_{12}Se_{60}$) condenser and.an objective turret with interchangeable germanium glass alloy lenses of numeric apertures of 0.56 and 0.85 (LightPath Technologies, Orlando, FL). This corresponds to effective FPA pixel sizes of 2.5 μm and 0.8 μm respectively. The lenses are coated with an anti-reflection coating (IR-3) that transmits approximately 98% of the incident beam at the QCL's center wavelength. Sample alignment and raster capabilities are controlled with a precision microscope stage (Prior Scientific, Rockland, MA). The instrument is configured in transmission mode with a liquid nitrogen cooled 128x128 pixel focal plane array (FPA) mercury cadmium telluride

(MCT) detector (IRCameras, Santa Barbara Focal Plane, Santa Barbara, CA). A 0.5 NA reflective Schwarzschild objective, oculars, and a CMOS camera were installed on the system for sample alignment.

2.2 Data Acquisition

To test the optical system, images were acquired for a USAF 1951 optical resolution target conforming to the MIL-STD-150A standard. This target has been traditionally used to test the performance of imaging systems. The target was patterned using SU-8 photoresist deposited at a thickness of 15 μm and developed on a 2mm thick barium fluoride (BaF_2) substrate (International Crystal Laboratory, Garfield, NJ). The imaged patterns are the bars at group 5 element 1 which has a standardized bar width of 15.63 μm. Frames from the FPA were collected at 1610 Hz with an integration time of 0.02 ms. The QCL was stepped through its entire frequency range from 1570 to 1738 cm^{-1} in 0.5 cm^{-1} steps, and for each band, 1600 frames were recorded by the FPA and co-added to generate each image in the sequence. At each wavenumber, the laser current was calibrated such that its detected power falls within the dynamic range of the FPA. The same process was performed on a blank BaF_2 surface to create a background spectrum. At each wavenumber, a background image was taken along with the target image. This was used to ratio out the spectral contributions from the source, atmosphere, and other systematic elements in order to calculate the SU-8 absorbance spectrum. Absorbance was then calculated by computing the negative base 10 logarithm of the target to background ratio.

Configuring the FPA and image acquisition was controlled by WinIR (IRCameras, Santa Barbara Focal Plane, Santa Barbara, CA). The image sequences were then processed and visualized using custom scripts written in MATLAB (The MathWorks, Nantucket, MA), ENVI (ITT Visual Information Solutions, Boulder, CO), and ImageJ (National Institutes of Health, Bethesda, MD).

The comparative FT-IR images were taken with a Varian 680-IR FT-IR spectrometer a 620-IR imaging microscope equipped with a 0.5 NA reflective Schwarzschild objective (Agilent, Santa Clara, CA). The Varian system also uses a liquid nitrogen cooled 128x128 pixel MCT FPA. The samples were measured at 2 cm^{-1} spectral resolution with 32 co-additions and the absorption spectrum was calculated based on a background frame obtained with a 128 co-additions.

3. RESULTS AND DISCUSSION

A comparison of images acquired with both the QCL and FT-IR imaging spectrometers are presented in figure 2. The results were compared with images taken by a Varian FT-IR system at the same sample location illustrating the spatial resolution of both systems at 1608 cm^{-1}. For this image the QCL based system used 0.56 NA germanium glass alloy objective and a matching condenser, while the Varian was fitted with a 0.5 NA reflective Schwarzschild objective. The image size over 128x128 pixels for the QCL instrument is approximately ~300 μm x 300 μm in our designed system, whereas the commercial system images an area of approx. ~ 700 μm x 700 μm.

As expected from a coherent source, features at the edges of the bars are especially apparent in the QCL images. The edge intensity at this wavenumber is roughly twice that of the actual SU-8 absorbance measurement from the center of the bar. This is likely due to multiple reflections and scattering from the structures in the sample, which is significantly more pronounced when using a spatially coherent source. In contrast, the absorbance profile is relatively flat across the entire width of the bar in the FT-IR image. With the use of a coherent source, fringing is visible in the background as well. Observing the 1710 cm^{-1} and 1650 cm^{-1} column images of Figure 4a, a broad semi-circular pattern is visible in the top right quadrant of the image. Additional finer fringe structures are present especially in the lower left quadrant. The magnitudes of these fluctuations are wavelength dependent.

Coherence effects can be seen more clearly in Figure 3 with images taken with a 0.85 NA objective with an effective pixel size 0.8 μm. The image of the target at group 5 element 3, with expected bar widths of 12.41 μm shows fringes contoured around the edges of the SU-8 on the sample. Here, we also imaged two 10 μm polystyrene spheres placed in close proximity to one another such that the interference pattern of the fringes could be observed. The theoretical concept behind this phenomenon is that, every pixel on the detector receives signal contributions from not only the corresponding pixel at the sample plane, but also pixels around it with a radius depending on the coherence area.[19] These electric field contributions interfere depending on phase and the result is seen as fluctuating intensities by the detector. Therefore, while these fringes may appear as noise, they actually contain structural information about the sample. A complete theoretical framework is required to understand the meaning and utility of this additional information provided by the QCL system in order to separate absorbance data from structural data.

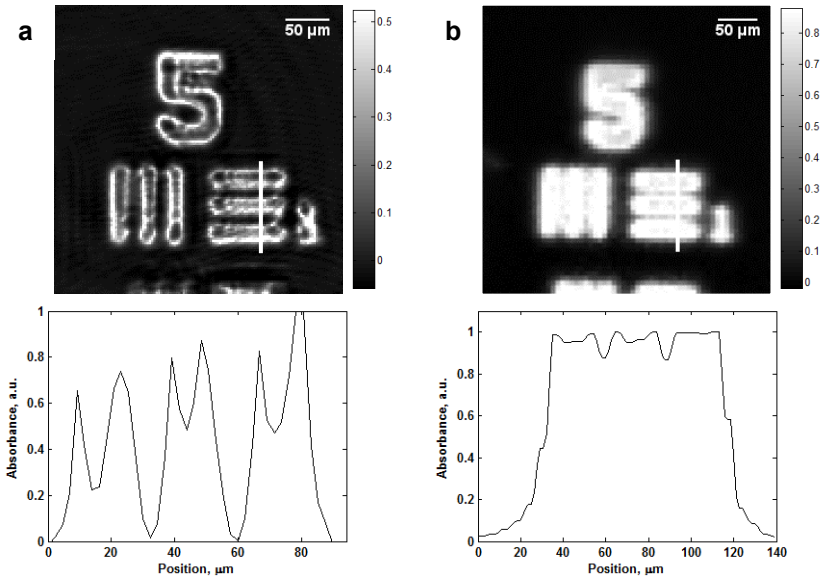

Figure 2. Absorbance images at 1606 cm^{-1} of a 1951 USAF resolution test chart (group 5, element 1) acquired by a a) QCL based system with a germanium glass alloy objective with a 0.56 NA, and b) Varian FT-IR system with a 0.5 NA Schwarzschild objective. SU-8 has an absorbance peak at this wavenumber as shown in Figure 5. The second row shows the profile across the horizontal SU-8 bars as indicated by the vertical line in the images. These absorbance values have been normalized in order to compare the images.

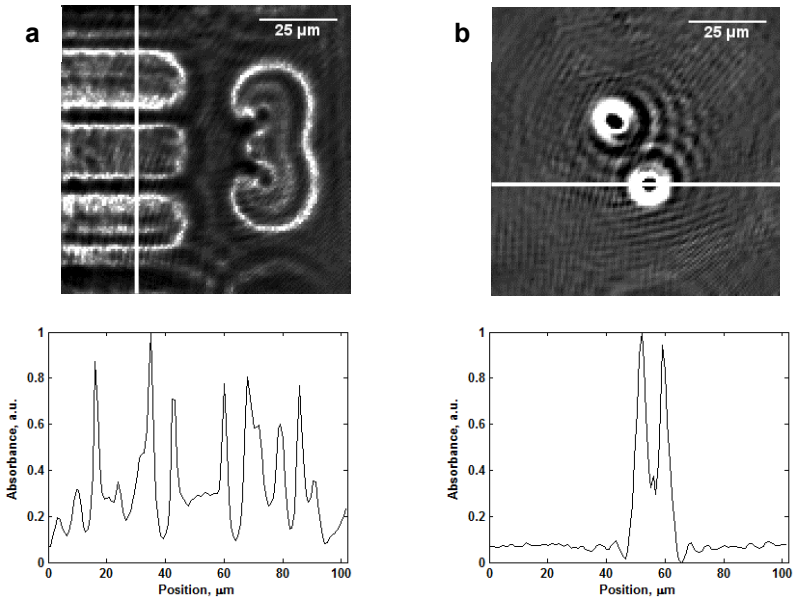

Figure 3. Interference patterns due to the effects of a coherent source a) SU-8 patterned USAF 1951 resolution target (group 5 element 3), and b) 10 µm diameter polystyrene spheres. The plots show the absorbance profile across the image in the region as indicated by the line. The effective pixel size is 0.8 µm making the field of view 102.4 µm in each dimension.

The SU-8 photoresist has distinctive absorbance peaks at 1608 and 1580 cm^{-1} while BaF_2 is transparent across the mid-infrared wavelength range. Figure 4 shows images at each of these absorbance peaks as well as images at 1650 and 1710 cm^{-1} where the spectral profile is flat. The lighter shading at 1608 cm^{-1}, indicating higher absorbance, is clear especially in the numeric five in both the QCL and FT-IR rows. Figure 5 shows the absorbance spectra measurements of SU-8 from the numeric five on the sample. This span from 1570 to 1738 cm^{-1} represents the tunable range of the QCL with the data taken at 0.5 cm^{-1} resolution. The FT-IR spectral data displayed here is only a subset of the full range (3850-0 cm^{-1} at 2

cm^{-1} resolution). These measurements demonstrate that a QCL based system can recover the SU-8 spectrum at these positions. However, we observe significantly more spectral noise.

Noise has a drastic impact on the signal to noise ratio (SNR) of the spectra and, consequently, on the quality of images acquired which lowers spatial and spectral quality, imaging speed, and the types of measureable samples. A contributing factor to noise comes from power fluctuations in the laser which have been measured up to 1.2 percent. Furthermore, laser speckle in the images has been measured at approximately 5 to 6 percent, though the effect is expected to be strongly sample-dependent. These issues become worse at the limits of the laser's tunable range as well as at select positions where atmospheric water absorption is strongest. These challenges must be addressed to make full use of the QCL's high flux advantage over the globar source used in FT-IR spectroscopy.

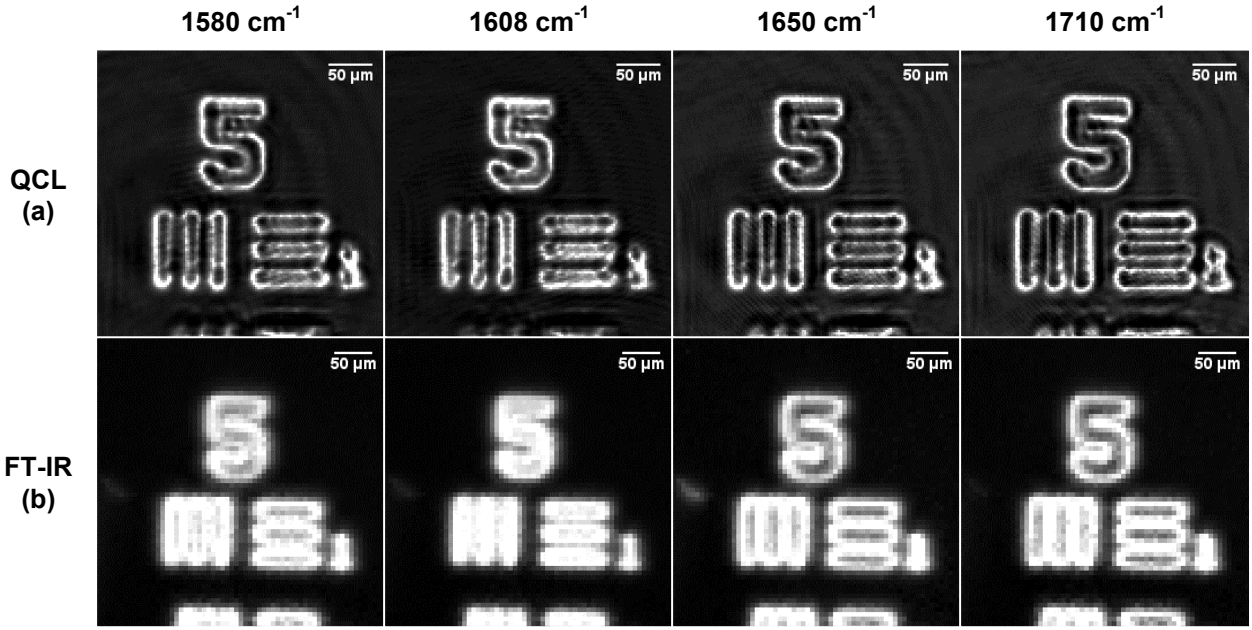

Figure 4. Absorbance images at select wavenumbers of a SU-8 patterned 1951 USAF resolution target (group 5, element 1) acquired using a) a QCL system equipped with a 0.56 NA objective, and b) a Varian FT-IR system with a 0.5 NA objective. The target consists of a SU-8 photoresist pattern on a BaF_2 substrate. SU-8 has absorbance peaks at 1580 cm^{-1} and 1608 cm^{-1} which can be seen by the lighter shading within the bars.

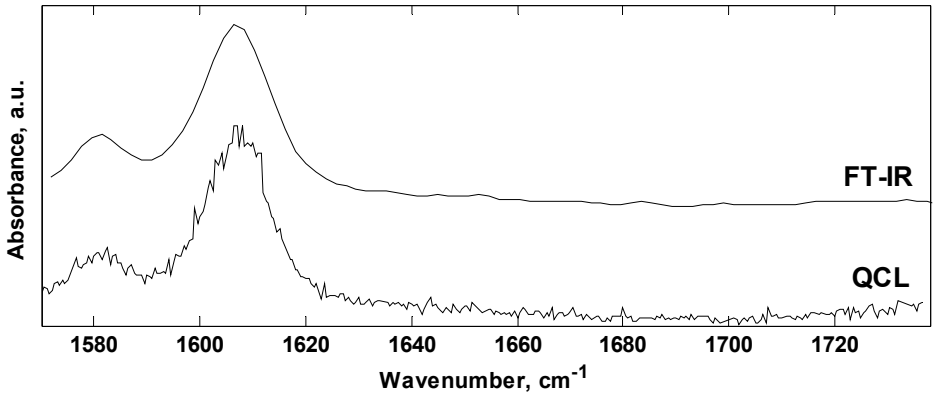

Figure 5. Absorption spectra of SU-8 photoresist measured by a QCL system and Varian FT-IR system at 0.5 cm^{-1} and 4 cm^{-1} spectral resolutions respectively. The spectra were calculated from a 3x3 pixel averaged window from the data shown above in Figure 4 and the values have been normalized for comparison.

The QCL model used in this instrument has a tunable wavelength of 168 cm^{-1} centered at 1650 cm^{-1}. This entire range corresponds to just a single band (Amide 1) found in tissues. Therefore, this instrument is not equipped to perform tissue diagnostics as imaging at multiple bands is required to provide contrast. The mid-infrared range spans roughly 4000 cm^{-1} and multiple QCL devices would need to be multiplexed together for adequate coverage. Even then, a full range measurement would not be feasible while FT-IR spectrometers are readily available. However, for sample diagnostics and imaging purposes, most the spectral data taken is not actually used; only a few spectral bands are needed to provide contrast.[25] In this case, however, an FT-IR spectrometer would first need to survey the spectrum and identify the spectral bands of interest. Then, a few separate QCL devices will tune to these bands and provide the spectral contrast required. Matching them to work in a seamless multiplexed configuration is an area of further development.

4. CONCLUSION

We have demonstrated the use of QCLs as a source for discrete frequency mid-infrared wide-field imaging. Their narrow spectral linewidths tunable to wavenumbers and high intensity emissions have many advantages to the globar source typically used in FT-IR spectroscopic imaging. The intrinsic properties of the QCL, especially the high spatial and temporal coherence, generate images that contain both absorbance (chemical) data as well as structural information and will require careful interpretation. The spatial resolution of the QCL system is competitive to that of a commercial FT-IR instrument, although more development is required to improve the noise characteristics in the spectral data. The advantage of a QCL based system lies with single wavelength measurements where it offers imaging speeds and intensities far higher than what a FT-IR instrument can provide.

ACKNOWLEDGEMENTS

This work was supported in part by the National Institute of Health under grant number 5R01EB009745-03. M.V. Schulmerich acknowledges support through Congressionally Directed Medical Research Program Postdoctoral Fellowship BC101112. The authors would like to thank Jui-Nung Liu for target sample preparation.

REFERENCES

[1] Bhargava, R., “Infrared spectroscopic imaging: the next generation,” Applied spectroscopy 66(10), 1091–120 (2012).
[2] Bhargava, R., Wang, S., and Koenig, J.L., “FTIR Microspectroscopy of Polymeric Systems,” Advances in Polymer Science 163, 137–191 (2003).
[3] Bhargava, R., “Towards a practical Fourier transform infrared chemical imaging protocol for cancer histopathology,” Analytical and Bioanalytical Chemistry 389(4), 1155–69 (2007).
[4] Kong, R. & Bhargava, R. "Characterization of porcine skin as a model for human skin studies using infrared spectroscopic imaging," The Analyst 136, 2359–66 (2011).
[5] Rao, G. N. & Karpf, A. "External cavity tunable quantum cascade lasers and their applications to trace gas monitoring," Applied optics 50, A100–15 (2011).
[6] Bhargava, R. & Kong, R. "Structural and biochemical characterization of engineered tissue using FTIR spectroscopic imaging: melanoma progression as an example," SPIE Proceedings 6870, 687004–687004–10 (2008).
[7] Griffiths, P., and Haseth, J.A. De, [Fourier transform infrared spectrometry, 2nd ed.], John Wiley & Sons, Hoboken, NJ, 560 (2007).
[8] Bhargava, R. & Levin, I. W. "Fourier transform infrared imaging: theory and practice," Analytical chemistry 73, 5157–67 (2001).
[9] Nasse, M.J., Walsh, M.J., Mattson, E.C., Reininger, R., Kajdacsy-Balla, A., Macias, V., Bhargava, R., and Hirschmugl, C.J., “High-resolution Fourier-transform infrared chemical imaging with multiple synchrotron beams,” Nature methods 8(5), 413–6 (2011).
[10] R.K. Reddy, M.J. Walsh, M.V. Schulmerich, P.S. Carney, R. Bhargava “High-definition infrared spectroscopic imaging” Appl. Spectrosc. 67, 93-105 (2013)
[11] Faist, J. et al. "Quantum Cascade Laser," Science 264, 553–6 (1994).

[12] Luo, G. P. *et al.* "Grating-tuned external-cavity quantum-cascade semiconductor lasers," Applied Physics Letters 78, 2834 (2001).
[13] Capasso, F. "High-performance midinfrared quantum cascade lasers," Optical Engineering 49, 111102 (2010).
[14] Wysocki, G. *et al.* "Widely tunable mode-hop free external cavity quantum cascade laser for high resolution spectroscopic applications," Applied Physics B 81, 769–777 (2005).
[15] Kosterev, A.A., and Tittel, F.K., "Chemical sensors based on quantum cascade lasers," IEEE Journal of Quantum Electronics 38(6), 582–591 (2002).
[16] Paldus, B.A., Harb, C.C., Spence, T. G., Zare, R.N., Gmachl, C., Capasso, F., Sivco, D.L., Baillargeon, J.N., Hutchinson, A.L., et al., "Cavity ringdown spectroscopy using mid-infrared quantum-cascade lasers," Optics letters 25(9), 666–8 (2000).
[17] Namjou, K. et al. "Sensitive absorption spectroscopy with a room-temperature distributed-feedback quantum-cascade laser," Optics letters 23, 219–21 (1998).
[18] Kolhed M. et al. "Assessment of quantum cascade lasers as mid infrared light sources for measurement of aqueous samples," Vibrational Spectroscopy 29, 7 (2001)
[19] Kole, M. R., Reddy, R. K., Schulmerich, M. V, Gelber, M. K. & Bhargava, R. "Discrete frequency infrared microspectroscopy and imaging with a tunable quantum cascade laser," Analytical chemistry 84, 10366–72 (2012).
[20] Phillips, M. C. & Ho, N. "Infrared hyperspectral imaging using a broadly tunable external cavity quantum cascade laser and microbolometer focal plane array," Optics Express 16, 1836–45 (2008).
[21] Guo, B., Wang, Y., Peng, C., Luo, G. P. & Le, H. Q. "Multi-Wavelength Mid-Infrared Micro-Spectral Imaging using Semiconductor Lasers," Applied Spectroscopy 57, 811–822 (2003).
[22] B.J. Davis, P.S. Carney, R. Bhargava "Infrared Microspectroscopy of Intact Fibers" Anal. Chem. 83, 525–532. (2011)
[23] B.J. Davis, P.S. Carney, R. Bhargava "Theory of mid-infrared absorption microspectroscopy. I. Homogeneous samples" Anal. Chem., 82, 3474–3486 (2010)
[24] B.J. Davis, P.S. Carney, R. Bhargava "Theory of mid-infrared absorption microspectroscopy. II. Heterogeneous samples" Anal. Chem., 82, 3487–3499 (2010)
[25] R. Bhargava, D.C. Fernandez, S.M. Hewitt, I.W. Levin "High throughput assessment of cells and tissues: Bayesian classification of spectral metrics from infrared vibrational spectroscopic imaging data" Biochim Biophys Acta. 1758, 830-845 (2006)